# POST-WILDFIRE DEBRIS FLOW THAT AFFECTED A RAILWAY AND HIGHWAY IN BC

Kaushal Gnyawali[1] & Dwayne D. Tannant[1]
[1] *University of British Columbia, Kelowna, BC, Canada*

GeoCalgary 2022 October 2-5 Reflection on Resources

ABSTRACT
A post-wildfire debris flow originating from the 2021 Lytton Creek wildfire in B.C. affected the community of Nicomen on August 16, 2021, during the first significant rainfall after the July wildfire. The First Nations village of Nicomen is located 14 km east of Lytton, along the Thompson River. The CP Railway and Highway 1 run along the edge of the Thompson River. The debris flow came down a small creek that passes under a road in Nicomen before descending to a sediment retention basin beside a railway embankment. The culverts under the railway usually deliver water to a vertical-drop intake structure that passes the water under Highway 1 and into the Thompson River. The debris flow washed out the road in Nicomen before proceeding downstream and blocking culverts under the railway and highway. The debris overtopped these structures, blocking two critical transportation routes. The transport and deposition process of the debris flow was simulated using a two-phase fluid model in r.avaflow using a high-resolution topographic model generated by processing images captured with a UAV during a field investigation. This paper compares the simulation results with field evidence of the passage and deposition of the debris and water.

RÉSUMÉ
Une coulée de débris post-incendie de forêt provenant de l'incendie de Lytton Creek en 2021 en Colombie-Britannique a touché la communauté de Nicomen le 16 août 2021, lors des premières pluies importantes après l'incendie de juillet. Le village des Premières nations de Nicomen est situé à 14 km à l'est de Lytton, le long de la rivière Thompson. Le chemin de fer du CP et l'autoroute 1 longent le bord de la rivière Thompson. La coulée de débris a descendu un petit ruisseau qui passe sous une route à Nicomen avant de descendre dans un bassin de rétention des sédiments à côté d'un remblai de chemin de fer. Les ponceaux sous la voie ferrée acheminent généralement l'eau vers une structure de prise d'eau à chute verticale qui fait passer l'eau sous la route 1 et dans la rivière Thompson. La coulée de débris a emporté la route à Nicomen avant de continuer en aval et de bloquer les ponceaux sous la voie ferrée et l'autoroute. Les débris ont recouvert ces structures, bloquant deux voies de transport critiques. Le processus de transport et de dépôt de la coulée de débris a été simulé à l'aide d'un modèle de fluide à deux phases dans r.avaflow à l'aide d'un modèle topographique à haute résolution généré par le traitement d'images capturées avec un UAV lors d'une enquête sur le terrain. Cet article compare les résultats de la simulation avec des preuves sur le terrain du passage et du dépôt des débris et de l'eau.

## 1 INTRODUCTION

The Lytton Creek wildfire started on June 30, 2021, one day after Canada's highest ever temperature (49.6 °C) was recorded at Lytton. The fire destroyed the village of Lytton and grew over the following weeks to cover an area of 83,740 hectares. Rainfall on August 16, 2021, triggered a post-wildfire debris flow in Thom Creek, which passes through the First Nations village of Nicomen, located 14 km east of Lytton, B.C. The debris flow also affected Highway 1 and the Canadian Pacific Railway along the Thompson River. Debris flows are known to increase for a few years after a wildfire (DeGraff et al., 2015). The likelihood of post-wildfire debris flows and floods increases in proportion to the burn severity and the percentage of a watershed burned (Jordan, 2015). This paper documents the physical impacts of this event and presents the results of a numerical simulation of the water and debris movement down the lower part of Thom Creek.

We conducted our field investigation on November 3, 2021. Two weeks later, a much more destructive debris flow occurred in Thom Creek associated with the devastating atmospheric river that affected many watersheds in B.C. We only document the August 16, 2021 debris flow in this paper. UAV imagery was collected and processed using Structure-from-Motion (SfM) software (Asghar and Tannant, 2018). Data from various sources are used. Lidar point cloud data from the fall of 2019 with a vertical accuracy of 0.14 m are available for the lower part of Thom Creek from LidarBC (LidarBC). Historical precipitation data were taken from the Lytton weather station, and radar precipitation images were obtained from the Silver Star Mountain station (Historical Radar). Sentinel-2 imagery was used to create a burn severity map. The watershed boundaries and streams were obtained from the Freshwater Atlas of B.C. (B.C. freshwater).

## 2 BIOGEOCLIMATIC ZONES AND TOPOGRAPHY

The bedrock geology consists of Permian to Triassic Mount Lytton Complex metamorphic rocks (Cui et al., 2017). Glacial tills, colluvium and talus dominate the surficial geology in the area.

The lower portions of the watersheds lie in a Ponderosa Pine biogeoclimatic zone, while the upper watersheds lie in the Interior Douglas Fir biogeoclimatic zone (BCMFR, 2007). The mean precipitation for August in the mid to upper watersheds near Nicomen is approximately 25 to 30 mm (ClimateBC_Map). The median maximum one-day precipitation in this area during August is 7 to 10 mm (climatedata.ca).

Figure 1 shows the topography and watershed boundaries for Thom Creek. The study area is located at the western edge of the Thompson Plateau. The topographic elevations range from 181 m at the Thompson River to 1400 m. The Thom Creek watershed has an area of 5.53 km$^2$, a relief of 1219 m. The mainstream of the creek is 3.67 km long. The Melton ratio, which is given by the watershed relief divided by the square root of the watershed area (Wilford et al. 2004), is 0.52.

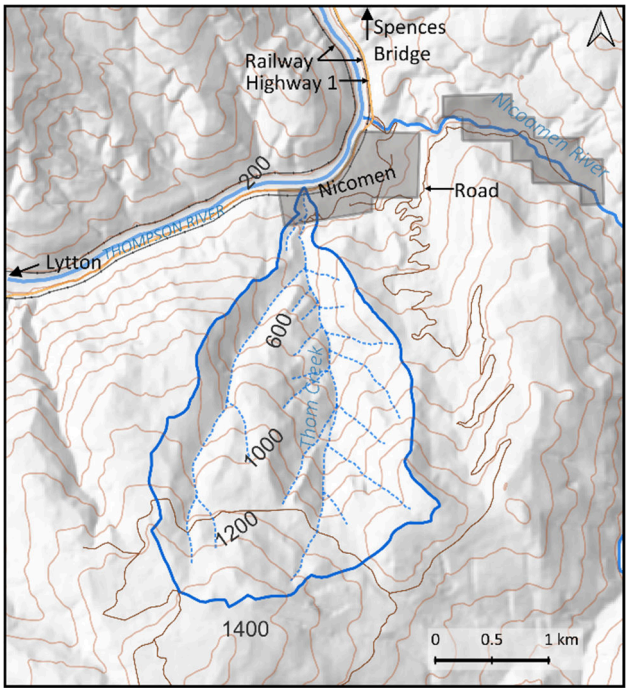


Figure 1. Topography and watershed boundary (blue)

The stream length and Melton ratio can be used to indicate the nature of the watershed response to a significant precipitation event. Figure 2 shows the expected response using the empirical regions defined by Church and Jacob (2020). The Thom Creek watershed falls within a zone where debris floods and debris flows occur.

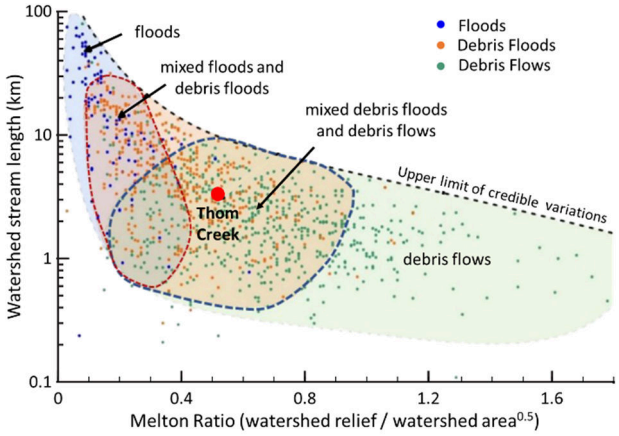


Figure 2. Expected response for Thom Creek during a significant runoff (after Church and Jacob, 2020)

## 3 LYTTON CREEK WILDFIRE AND BURN SEVERITY

We used Sentinel 2 cloud-free imagery of the Nicomen area to estimate the wildfire burn severity arising from the Lytton Creek wildfire using Normalized Burn Ratio (NBR) in pre- and post-fire images (Petropoulos et al., 2014). The selected images were from June 26 and August 28, 2021. Figure 3 shows the calculated pattern of burn severity, with roughly 40% of the Thom Creek watershed experiencing moderate to high burn severity resulting from the Lytton Creek wildfire. The upper and eastern sides of the watershed had the highest burn severity.

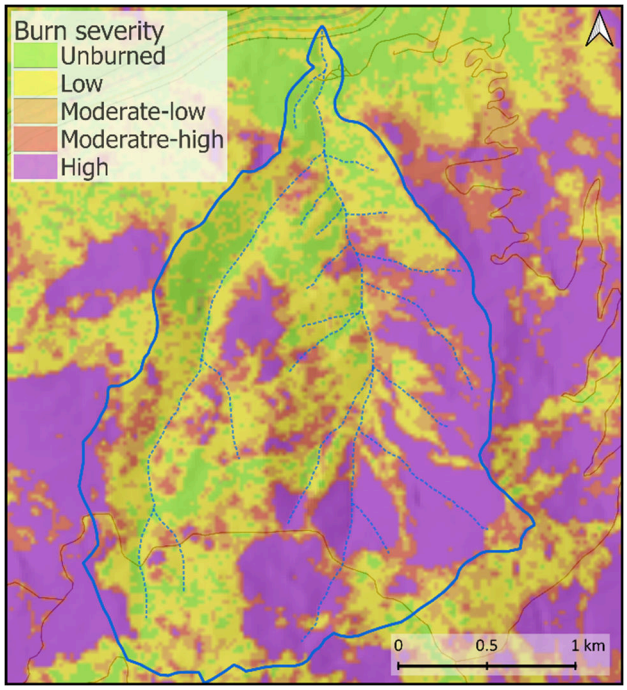


Figure 3. Burn severity map based on analysis of Sentinel 2 satellite images

## 4 PRECIPITATION ON AUGUST 16, 2021

On August 16, 2021, widely distributed rainfall passed over south-central B.C. This was the first period of significant rainfall after the fire. The Lytton RCS weather station recorded 16.5 mm of rain on August 16. A plot of rainfall intensity taken from historical radar images collected by the Silver Star station (10-minute intervals) is shown in Figure 4. The radar images showed localized rainfall in the Nicomen area starting at 11:00 with peak intensities of ~6 mm/hour at 15:00 and 19:30 PST. The radar data for the small watersheds in the Nicomen area indicated that at least 12 mm of rain fell within 7 hours.

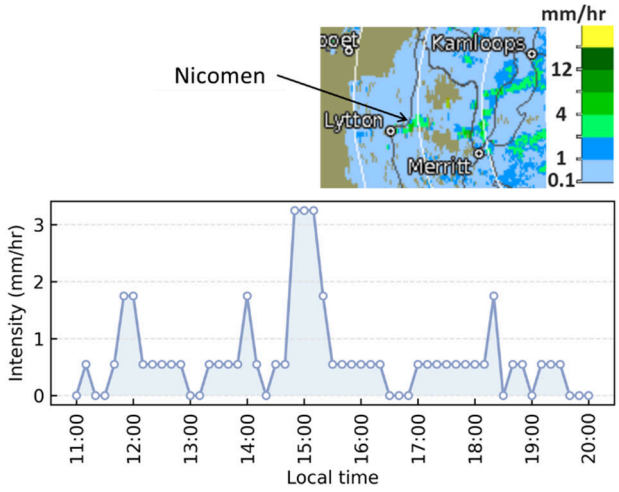


Figure 4. Hourly rainfall intensity on August 16, 2021, and precipitation distribution at 15:00 local time.

## 5 DRONE-BASED MAPPING AND ANALYSIS

An orthophoto of Thom Creek, where it enters the Thompson River, is shown in Figure 5. More detailed orthophotos with 1 m contour lines are shown in Figures 6 to 8. These orthophotos were created from drone images acquired on November 3, 2021. The rainfall triggered a debris flood or flow that first washed out an access road in Nicomen (Figure 6) before descending 62 m in elevation over a 215 m horizontal travel distance through a small bedrock canyon with waterfalls. The creek exits the canyon and enters a small retention basin (Figure 7) which had an approximate storage volume of 1100 $m^3$ based on an analysis of 2019 lidar data.

A pair of vertically stacked culverts starts near the bottom of the retention basin and passes through the CP Railway embankment. The lower culvert was probably installed when the railway was first built and consists of a concrete or masonry box culvert that is roughly 1 m wide and slightly taller. This culvert was extended southward by adding a 1.2 m diameter corrugated steel pipe (CSP) when the railway was converted to twin tracks. Another 1.2 m diameter CSP was stacked above the old culvert (likely when the track was twinned) to handle storm events. However, these two culverts were not sufficient to pass the water and debris on August 16, and the retention basin filled with debris and the track was overtopped.

Water and debris that passed over the railway and through the railway culverts (Figure 7) overwhelmed a grated vertical drop structure to a drain under the highway (Figure 8). The debris fanned out across the highway and was partially retained by a ~0.6 m high concrete barrier that runs along the northern shoulder of the road. This barrier is an upward extension of a vertical concrete retaining wall that separates the highway from the Thompson River. The exposed height of the wall at the drain under the highway is approximately 4.5 m.

Vertical profiles taken along the creek and through the railway and highway embankment are shown in Figure 9. The data were obtained from a 2019 lidar survey and an SfM-derived point cloud using November 3, 2021 photos. Below the waterfalls, the creek flows at a gradient of 19% (11°) into the retention basin. The railway track on the embankment is 6.5 m higher than the invert of the lowest culvert and is 16 m higher than Highway 1 immediately to the north of the railway. The culverts through the railway embankment have a gradient of 14% (8°). The black dashed line in Figure 9 indicates the expected storage capacity for the debris retention basin.

Differences between the 2019 lidar data and the 2021 SfM data show areas where (1) erosion had occurred upstream of the debris basin, (2) debris was deposited in the upper part of the debris basin (and not cleaned out), and (3) sediment was deposited along the Thompson River shore.

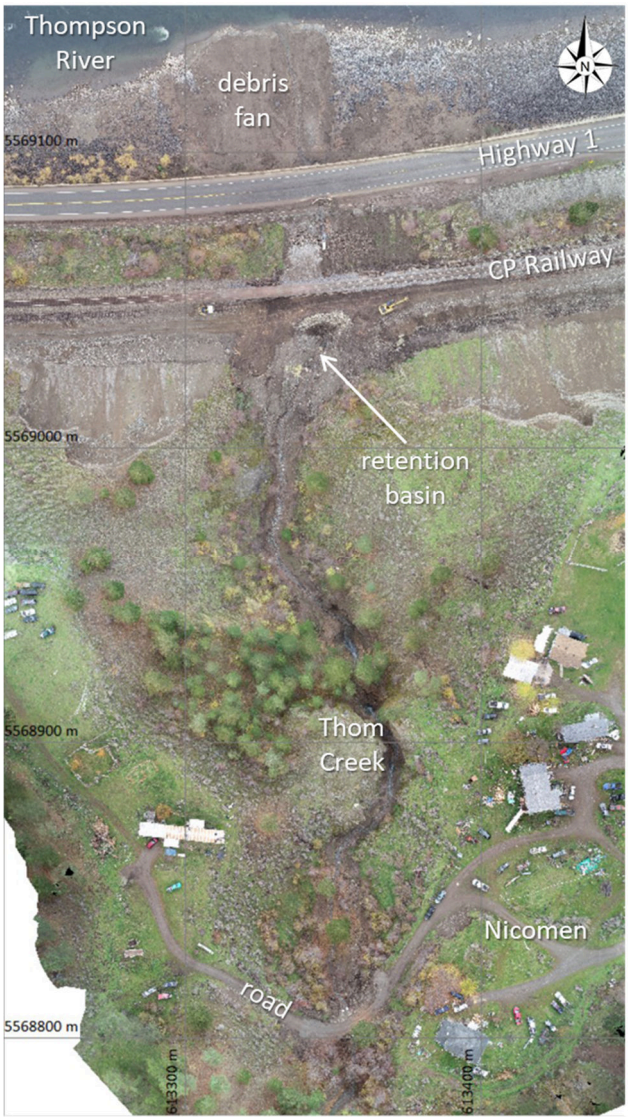


Figure 5. Orthophoto of the lower reach of Thom Creek (November 3, 2021)

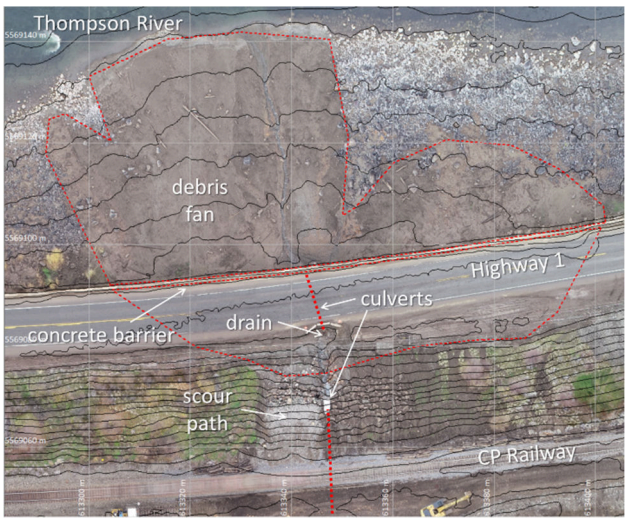


Figure 6. Area where Thom Creek passes under Highway 1 and enters the Thompson River

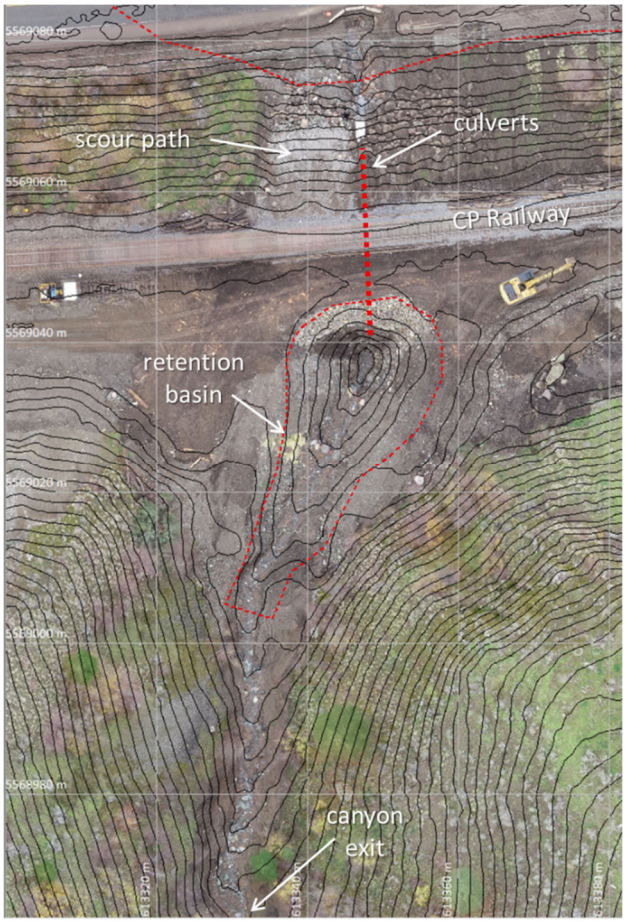


Figure 7. Area where Thom Creek passes through a sediment retention basin and the CP Railway

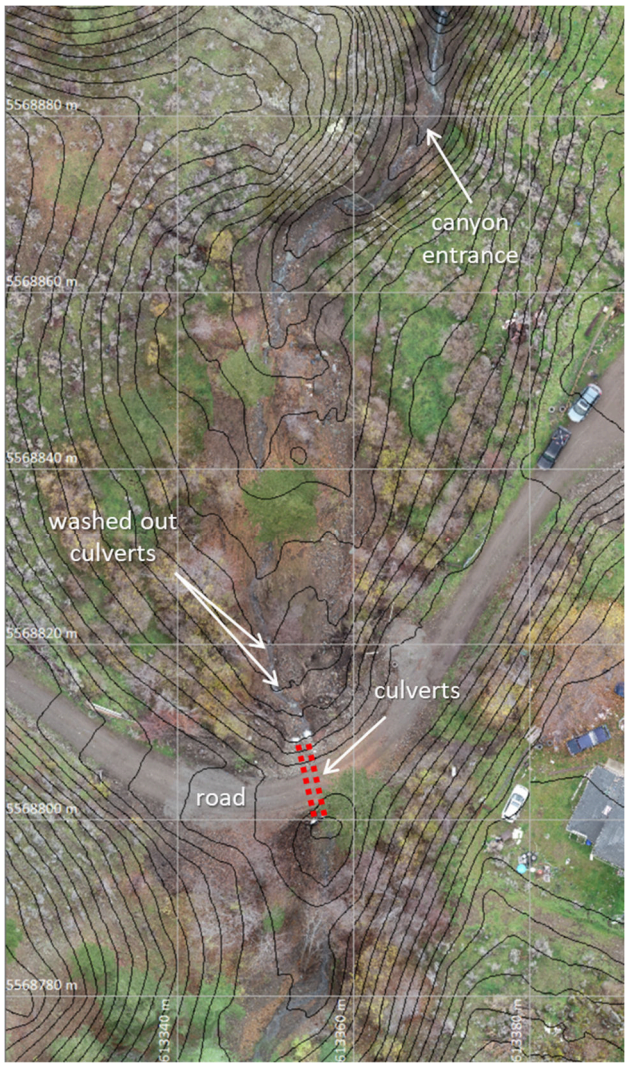


Figure 8. Area where Thom Creek passes under the road in Nicomen

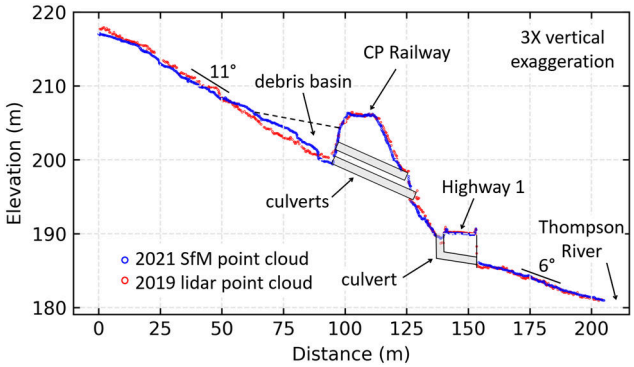


Figure 9. Vertical profile along the creek and culverts

The debris on the highway covered an approximate area of nearly 1500 m$^2$. The concrete barrier itself was also overtopped, and debris flowed down to the river forming a fan deposit. The surface area of the fan at the time of the site visit was roughly 3200 m$^2$. Little river erosion of the

sediment fan occurred between August 16 and the November 3 site visit because Thompson River only rose once above the water level recorded on August 16, and by only 0.1 m. The major floods in B.C., which also affected the Thompson River, occurred less than two weeks after the fieldwork.

The volumes of debris deposited within the region covered by Figure 5 were approximately 2000 $m^3$ upstream of the railway, 1000 $m^3$ on the highway, and at least 1500 $m^3$ on the fan and into the Thompson River. The total debris volume and the area of inundation and deposition rank this event as size class 3 using the Jakob (2005) size classification for debris flows, with an estimated peak discharge rate in the range of 3 to 30 $m^3/s$.

## 6 DEBRIS FLOW HYDROGRAPH

The inflow discharge and velocity hydrograph for this event at a location slightly upstream of the road through Nicomen was estimated as input to a numerical simulation of the debris flow travelling down the lower portion of the creek channel. Several methods exist to estimate the hydrograph (Mitchell et al., 2022). We approximated it as an idealized triangular hydrograph defined by the peak discharge ($Q_p$), the total inflow duration ($t_{in}$), and the time to peak ($t_p$), with the total volume (*Vol*) defined by the area of the triangle. The total inflow duration of the hydrograph can be obtained by dividing *Vol* by the area of the hydrograph. The peak was assumed to occur at a 20% lag time (i.e., $t_p$ = 20% of $t_{in}$).

In this study, we used the equation based on Froude similarity from Rickenmann (1999) to empirically estimate the peak discharge:

$$Q_p = c(Vol)^{5/6} \quad [1]$$

where *c* is a constant that ranges between 0.001 and 1, with values of 0.01 typical of muddy flows and 0.1 typical of granular flows (Ikeda et al., 2019). For this site, *Vol* = 4500 $m^3$ (constrained from field observations). The value of *c* = 0.01 because the debris flow had a muddy texture. Using these values, $Q_p$ was calculated to be 11 $m^3/s$, which falls within the empirical range noted by Jakob (2005) for a class 3 debris flow.

The debris flow velocity (*v*) varies over the inflow duration and was estimated using the following equation from Rickenmann (1999) for a location above the road in Nicomen.

$$v = 2.1Q^{0.33}S^{0.33} \quad [2]$$

The instantaneous discharge is *Q* and *S* is the channel slope (%). Figure 10 shows the estimated inflow and velocity hydrograph in Thom Creek above the road in Nicomen, approximately 275 m upstream from the culverts under the CP Railway.

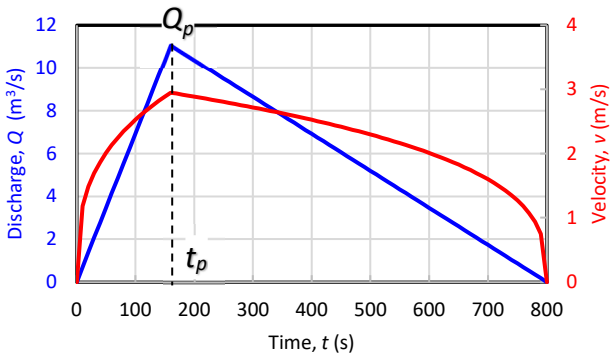


Figure 10. Estimated debris flow discharge and velocity hydrograph where Thom Creek passes the Nicomen road.

## 7 CULVERT CAPACITY

Thom Creek passes through culverts under a road in Nicomen and the CP Railway embankment. The debris flow washed out a pair of 300 to 400 mm diameter culverts at the road, and these were replaced by a pair of 900 mm diameter culverts. In both cases, the culvert slope was approximately 12%, and their length was 10 m.

Using a culvert analysis spreadsheet (USDA, 2022), the discharge capacity of the corrugated metal culvert (for water) was estimated assuming a projecting thin edge inlet and a Manning's *n* value of 0.024. An upstream water depth of 1.6 m was assumed above the culvert invert level, which corresponds to the point at which the road begins to be overtopped by water. The estimated flow capacity was only 0.2 to 0.35 $m^3/s$ for each original culvert. After they were replaced by 900 mm culverts, the flow capacity per culvert increased to 1.7 $m^3/s$ (3.4 $m^3/s$ for the pair), which is still well below the estimated peak discharge for the debris flow (11 $m^3/s$). This illustrates how vulnerable roads with in-stream culverts are to post-wildfire debris flows.

At the CP railway, the culvert slope was 14%, and each culvert had an approximate 1.2 m diameter and a length of 30 m. The lower culvert could be submerged in up to 6.5 m of water before the retention basin was filled and the tracks began to be overtopped. The lower culvert's estimated flow capacity was 6 $m^3/s$. The culvert stacked vertically above would have a lower capacity due to a lower submerged depth. Their combined capacity was estimated to be roughly 11 $m^3/s$ for clean water, which happens to match the estimated peak discharge for the debris flow. However, during a debris flow, the debris and logs carried down the creek can easily block culverts rendering them far less efficient.

## 8 DEBRIS FLOW SIMULATION

We used r.avaflow to simulate the debris flow. It is an open-source and GIS-based computational framework to simulate mass movements from a defined source area down the topography to a deposition area (Mergili et al., 2017). A three-phase numerical model using properties of the solids, fines, and fluid phases was set up in r.avaflow (Pudasaini and Mergili, 2019). The code has been

successfully used to simulate large landslides and avalanches, while its implementation for small debris flows is limited. This study tests r.avaflow on a terrain model with a 2 m grid size.

The simulation results are sensitive to the density ($\rho$), basal friction ($\delta$), and internal friction ($\phi$) assigned to the three phases. For this initial work, the following values were used for the solids, fines, and water phases, respectively.

$\rho$ = (2650,1800,1000) kg/m$^3$

$\delta$ = (10°, −, −)

$\phi$ = (35°, −, −)

The model did not consider kinematic viscosity, and other parameters were kept at default values, as defined in Mergili et al. (2017). While other combinations of parameters could have been used, a sensitivity analysis was beyond the scope of the present work.

A typical debris flow is a poorly sorted mixture of sediment and water that commonly contains 40 to 80% solids by volume (Iverson, 1997). For the simulation, a 25%, 25%, and 50% proportion by volume was assumed for the solids, fines, and water proportions, respectively.

The discharge hydrograph was simulated by releasing the debris flow over a 15 m wide cross-section of Thom Creek located 10 m upstream from the Nicomen road. Figure 11 shows the maximum flow velocity and the maximum flow height determined with the r.avaflow simulation.

The simulation captures the sediment deposition in the retention basin and high flow velocities in the steep canyon. High flow velocities were also predicted for outside bends in the steep channel leading to the retention basin. The velocities obtained in channelized portions are close to that simulated using HEC-RAS, a 2-dimensional numerical modelling software (BGC, 2021). High-velocity regions correspond to potential areas where material can be entrained by the debris flow from the channel base or sidewalls. However, including entrainment in the simulation is beyond the scope of the present work.

Despite the numerical simulation ignoring the presence of the two culverts under the railway embankment, the lateral extents of the debris deposition were similar to field observations, with the debris spreading out along the upstream side of the railway embankment and on the highway. The numerical model underestimated the depth of debris deposition on the highway and the fan along the Thompson River shore. The model predicted flow velocities down the northern side of the railway embankment in the range of 4 to 6 m/s. This area matches a downstream zone of scouring on the railway embankment that occurred when the debris flow overtopped the railway tracks.

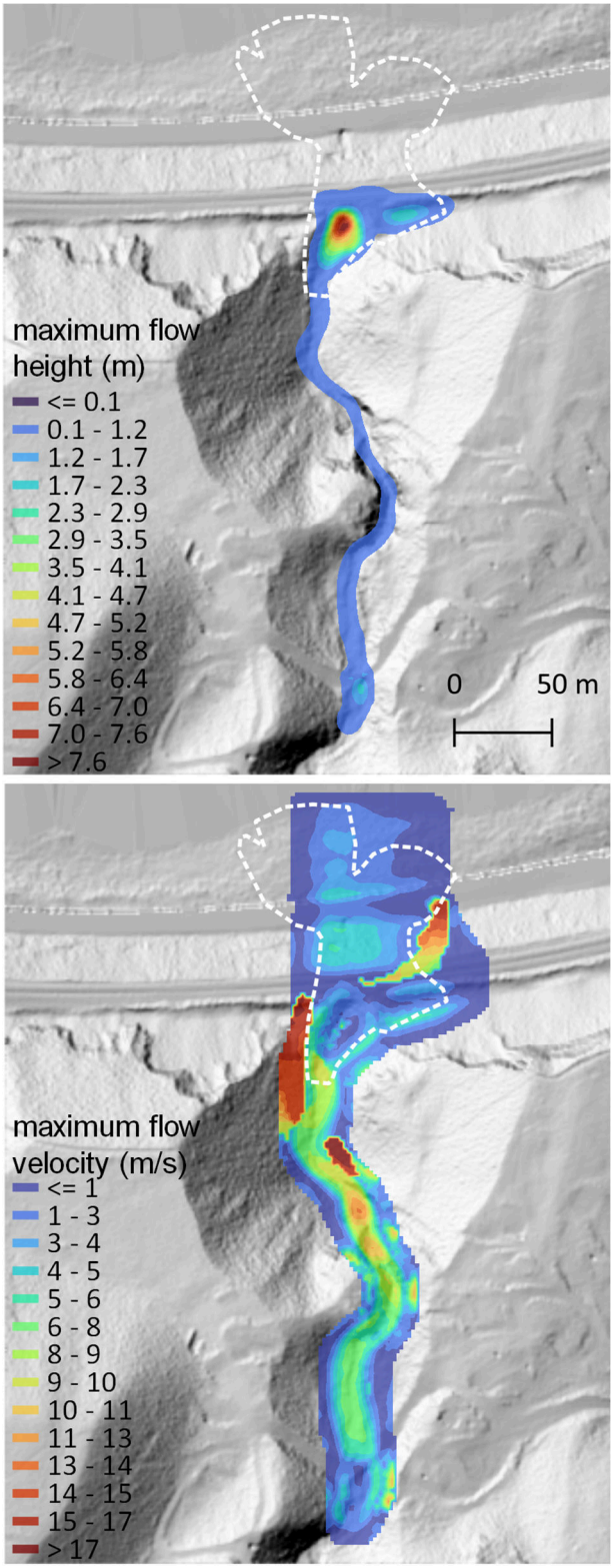


Figure 11. r.avaflow simulation results for the maximum flow height and velocity using a 2 m Lidar BC pre-event terrain. Flow heights are measured perpendicular to the slope, and the maximum flow velocity is a weighted average of all phases during the simulation.

## 9 CONCLUSIONS

This paper documents an August 2021 debris flow in the Thom Creek watershed that was burned a month earlier by the 2021 Lytton Creek wildfire.

Sentinel 2 satellite images were used to create a burn severity map, and doppler radar images were used to estimate the peak rainfall intensity associated with the debris flow. Aerial images of the lower watershed were taken with a drone. These images were processed with structure-from-motion photogrammetry software to create a post-event point cloud and orthomosaic and were compared with pre-event lidar data to measure features of interest.

From an analysis of the created maps, point clouds, and orthomosaic, the estimated volume of debris deposited near the creek's confluence with the Thompson River was at least 4500 $m^3$. The deposition volume and watershed characteristics provided insight into the possible peak discharge rate for the debris flow (11 $m^3/s$). These estimates provided input into numerical simulations of the debris flow passage through the lower part of the creek and can also aid in selecting appropriate culvert sizes.

## ACKNOWLEDGEMENTS

Tom Millard from the B.C. Ministry of Forests, Lands, Natural Resource Operations and Rural Development organized the site visit with Norman Drynoch, the Chief of the Nicomen Indian Band. Their help is gratefully acknowledged.

## REFERENCES

Asghar, U. and Tannant, D.D. 2018. Landslide mapping from structure-from-motion analysis of photos acquired by a drone. *7th Canadian Geohazards Conference*, Canmore. 9 p.

B.C. Freshwater. 2022. Freshwater Atlas. https://www2.gov.bc.ca/gov/content/data/geographic-data-services/topographic-data/freshwater

BCMFR. 2007. Tree Book: Learning to Recognize Trees of British Columbia. B.C. Ministry of Forests and Range. http://www.for.gov.bc.ca/hfd/library/documents/treebook/index.htm

BGC Engineering Inc. (BGC). 2021. Post-wildfire geohazard risk assessment: Lytton creek fire (K71086). Report prepared for the Ministry of Forests, Lands and Natural Resource Operations and Rural Development (MFLNRORD).

Church, M., & Jakob, M. (2020). What is a debris flood? *Water Resources Research*, 56(8): e2020WR027144.

ClimateBC. 2021. ClimateBC_Map – A interactive platform for visualization and data access. http://www.climatewna.com/ClimateBC_Map.aspx

Climatedata. 2022. https://climatedata.ca/

Cui Y., Miller D., Schiarizza P., and Diakow L.J. 2017. British Columbia digital geology. B.C. Ministry of Energy, Mines and Petroleum Resources, British Columbia Geological Survey Open File 2017-8, 9 p. Data version 2019-12-19

DeGraff J.V., Cannon S.H. and Gartner J.E. 2015. The timing of susceptibility to post-fire debris flows in the Western United States. *Environmental & Engineering Geoscience*, 21(4): 277-292.

Historical Radar. 2022. Canadian Historical Weather Radar. https://climate.weather.gc.ca/radar/index_e.html

Iverson, R. M. 1997. The physics of debris flows. *Reviews of Geophysics*, 35(3): 245-296.

Jakob M. 2005. A size classification for debris flows. *Engineering Geology*, 79: 151-161.

Jordan P. 2015. Post-wildfire debris flows in southern British Columbia, Canada. *International Journal of Wildland Fire*, 25(3): 322-336.

LidarBC. 2022. Open LiDAR Data Portal. https://governmentofbc.maps.arcgis.com/apps/MapSeries/index.html?appid=d06b37979b0c4709b7fcf2a1ed458e03

Mergili, M., Fischer, J. T., Krenn, J., & Pudasaini, S. P. 2017. r.avaflow v1, an advanced open-source computational framework for the propagation and interaction of two-phase mass flows. *Geoscientific Model Development*, 10(2): 553-569.

Mitchell, A., Zubrycky, S., McDougall, S., Aaron, J., Jacquemart, M., Hübl, J., Kaitna, R., and Graf, C. 2022. Variable hydrograph inputs for a numerical debris-flow runout model, *Nat. Hazards Earth Syst. Sci*. Discuss. [preprint]

Petropoulos G.P., Griffiths H.M., and Kalivas D.P. 2014. Quantifying spatial and temporal vegetation recovery dynamics following a wildfire event in a Mediterranean landscape using E.O. data and GIS. *Applied Geography*, 50: 120-131.

Pudasaini, S. P., & Mergili, M. 2019. A multi-phase mass flow model. *Journal of Geophysical Research: Earth Surface*, 124(12): 2920-2942.

Rickenmann, D. 1999. Empirical relationships for debris flows. *Natural Hazards* 19: 47–77.

USDA. 2012. United States Department of Agriculture-Natural Resources Conservation Service. Culvert analysis spreadsheet. Accessed from: https://www.nrcs.usda.gov/wps/PA_NRCSConsumption/download/?cid=nrcseprd329821&ext=xlsm

Wilford, D.J., Sakals, M.E., Innes, J.L., Sidle, R.C. and Bergerud, W.A. 2004. Recognition of debris flow, debris flood and flood hazard through watershed morphometrics. *Landslides* 1(1): 61-66.